Computational Studies of Possible Transition Structures in the Insertion and Windowing Mechanisms for the Formation of Endohedral Fullerenes

E. Sanville and J. J. BelBruno*

Department of Chemistry and Center for Nanomaterials Research, Dartmouth College, Hanover, New Hampshire 03755

Received: February 28, 2003; In Final Form: May 29, 2003

The possible structures involved in the ring penetration and windowing mechanisms for the formation of endohedral fullerenes are reported. Results for $X@C_{60}$ relaxed transition structures and energy barriers are reported, where X = H, He, N, NO, P, and As. The applicability of a mechanism to formation of a particular endohedral species is readily judged on the basis of these barriers, with only hydrogen, helium, and nitrogen as likely participants in direct insertion. Windowing was shown to be feasible only for hydrogen or nitrogen atoms under the adiabatic conditions of the calculations.

Introduction

Since the discovery of fullerenes, it has been shown that certain atoms and molecules could be inserted into the cage structure of fullerene molecules to form endohedral complex structures. Recently, it has been shown that nitrogen atoms may be inserted into the C_{60} cage structure and that $N@C_{60}$ may be produced in practical quantities using an atomic nitrogen beam impacting on a fullerene substrate. The endohedral material could be separated from the mixture with the parent fullerene by chromatographic techniques and was stable as a reagent in organic synthesis.[1−5] Although the phosphorus analogue could be produced using a similar beam impact technique, the $P@C_{60}$ complex was not long-lived and was not stable as a reagent in organic synthesis.[3] The arsenic analogue has not been reported. As expected from such an experiment, the yields of product are very low. Attempts to produce larger quantities of endohedral complexes involved the arc-discharge method, routinely used for bulk production of the parent fullerene. When applied to the production of endohedral fullerenes, this results in yields of less than one part per thousand of all fullerenes. Subsequently, high-pressure, high-temperature techniques[8,9] have increased the yield of endohedral fullerene as a fraction of fullerene production to approximately 0.1%.

Computational studies have been reported for the energetic stability and structure of these endohedral Group V complexes,[6] as well as the $H@C_{60}$ complex.[7] No computational studies have been reported, however, for possible transient structures present during the formation of these endohedral complexes. Such a study is important to improvements in the understanding of the formation process and, subsequently, to development of processes that might improve yields. Indeed, some uncertainty still exists as to the exact nature of the insertion mechanism for a specific endohedral species. It has been reported that different endohedral species escape the fullerene cage via different routes.[10] For example, metals and noble gases appear to remain trapped in the fullerene as it decreases in size through loss of C_2 units; the so-called "shrink-wrap" mechanism. Nitrogen atoms leave an intact C_{60} cage. Three possible endohedral insertion mechanisms have been recognized.[11] These include: ring penetration or direct insertion[12,13] of the species by passage through a pentagonal or hexagonal ring; windowing[14] or breaking of sufficient carbon−carbon bonds to create a large opening in the cage which subsequently re-closes after endohedral insertion, and the hole mechanism[11] or windowing in which at least one carbon−carbon bond does not re-close. There are no previously reported studies of the molecular structures involved in the three mechanisms. This report explores the possible structures that are consistent with formation of the complexes by means of the first two mechanisms. We evaluate the energetics and stability of the structures as well as the feasibility of endohedral complex formation through such structures.

Computational Methods

The use of ab initio theories with typical basis sets such as 6-31G* is extremely CPU intensive for the large systems under investigation here, even for single point calculations. The required CPU time tends to be highly sensitive to initial endohedral atom placement, with some points, including those very near to the optimized geometry, requiring substantial convergence time. Density functional theory calculations, using the B3LYP functional with the same basis sets, require even more CPU time. For these reasons, partial Hartree−Fock optimizations for direct insertion transition states were performed on each complex using the 3-21G* basis set. The SCF calculations used the quadratic convergence method to facilitate convergence for X = N and P, which were difficult cases. For the final energy calculations (for direct insertion) involving points at the extrema of the potential energy surface connecting reactants and products, B3LYP density functional theory was used with the 6-31G** basis set and the bond-optimized fullerene geometry from the lower level calculations. In all of these calculations, the bond angles were fixed at the experimental values of the parent fullerene. The windowing calculations employed the PM3 semiempirical model, but full optimization was completed at each separation distance. All calculations employed the GAUSSIAN 98 suite[15] of programs.

Results and Discussion

Direct Insertion Mechanism. For direct insertion of the endohedral species, the process is most likely to proceed through

* Corresponding author.

10.1021/jp030289h CCC: $25.00
Published on Web 07/24/2003

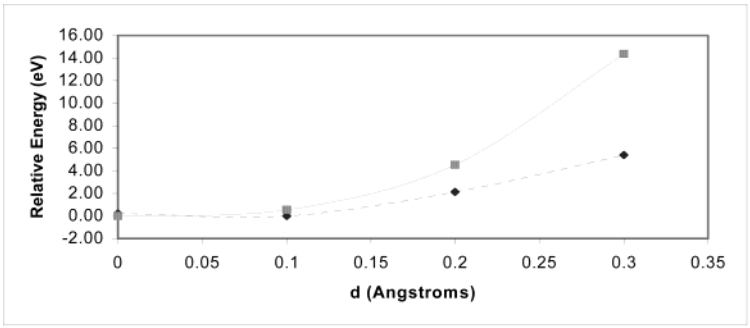

(a)

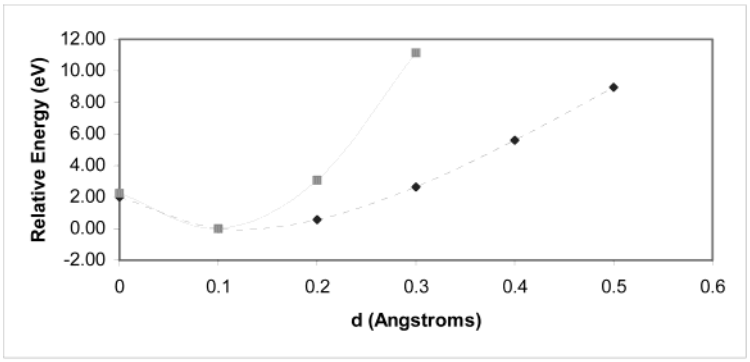

(b)

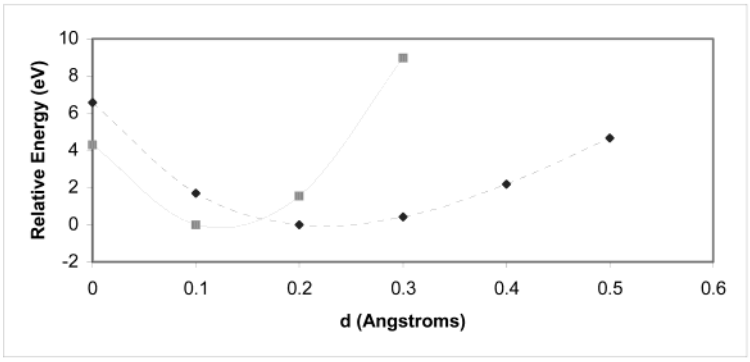

(c)

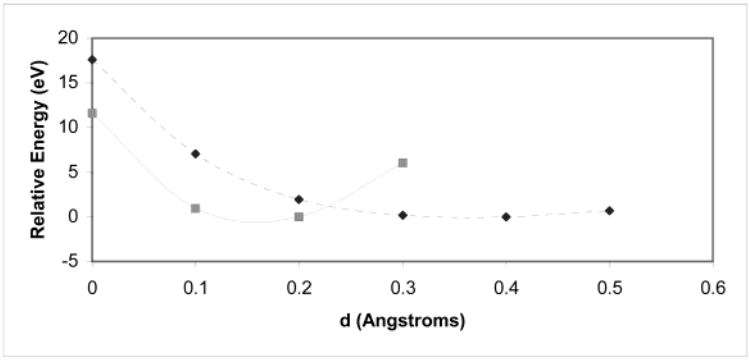

(d)

Figure 1. Potential energy as a function of ring expansion distance for a C_{60} surface hexagonal ring with a central X (solid line), and for benzene with a central X (dashed line), where X = H (a), He (b), N (c), and P (d), respectively. Calculations performed using the B3LYP/6-31G* method.

a structure in which the entering species is located in the center, or close to the center, of a hexagonal ring in the C_{60} cage structure. This pathway would provide the largest natural opening for insertion. The energy of this configuration, with the endohedral atom in the plane of the fullerene surface relative to that at infinite separation would provide an estimate of the effective barrier for formation of the endohedral fullerene via, for example, soft molecular beam bombardment, assuming for that experimental arrangement that the species travels through the surface of the C_{60} molecule rather than breaking any bonds. In the study of this mechanism, the formation of uncharged X@C_{60} was examined, where X = H, He, N, NO, P, and As. The extrema of the slice through the potential energy surface were taken as the infinite separation point, defined as the point of zero C_{60}-atom interaction energy, and the final inclusion of the atom inside the fullerene cage. Subsequently, the maximum energy structure, the prospective transition state for insertion, along the pathway was examined. Here, the endohedral species was placed in the center of a six-membered ring in a C_{60} molecule having the experimental parent fullerene geometry. This initial structure was then partially optimized under various selected geometric constraints to obtain the prospective transition structure. A series of single point energy calculations was performed while varying the distance of the endohedral species

TABLE 1: Minimal Energy Ring Expansions for a C_{60} Surface C_6 Ring with a Central Species X, the Same Arrangement for an Isolated Benzene Ring, and the van der Waals Radii for X

X	C_{60} expansion, Å	benzene expansion, Å	vdW radius, Å
H	0.030	0.050	1.20
He	0.093	0.127	1.40
N	0.124	0.225	1.55
P	0.160	0.336	1.80
As	0.193		1.85

outside of this calculated relaxed C_{60}, to establish a plot of potential energy versus distance from the C_{60}. The potential energy difference between the relaxed transition state and the separated species state was then calculated using a larger basis set and DFT method to estimate the energy barrier to endohedral C_{60} formation. Several different variations of this procedure were implemented and are described, along with the relevant results, in this section.

B3LYP/6-31G* calculations were initially performed on model structures formed by placing the endohedral species in the center of a benzene ring. A series of single point energy calculations as a function of ring expansion with fixed bond angles was used to estimate the optimum expansion distance, essentially the extent of flexing, of the target ring. These were followed by model calculations in which a hexagonal ring of C_{60} was flexed in a similar fashion. The calculations were run on a series of structures where the expansion of only a single surface ring was increased from 0.0 to 0.3 Å in increments of 0.01 Å, while maintaining the remaining bond lengths and all angles at the experimental values. The minimum energy in this expansion potential for both sets of these model calculations are summarized in Table 1 and shown graphically in Figure 1. The minimal relaxation distance is smaller, in all cases, for the C_{60} surface ring than for benzene, presumably due to unfavorable bond compression between nearest neighbor carbon atoms and next-nearest neighbor carbon atoms. As expected, the minimal relaxation expansion distances increase with increasing atomic van der Waals radii. As an initial entry point to the barrier for endohedral atom insertion, a series of single point calculations were performed to establish a potential energy curve with respect to the distance between the C_{60} cage with the single expanded ring as indicated in Table 1 and the endohedral species X. A curve of energy versus "reaction progress" for endohedral C_{60} formation via an insertion-like mechanism with the fixed optimal ring expansion for X = H, He, N, and P was obtained. These curves are shown in Figure 2. The estimated energy barriers derived from the curves are shown in Table 2.

To produce a transition state structure more closely resembling that expected for the impact mechanism, partial optimizations involving all fullerene cage bond distances, with angles remaining fixed at the experimental values, were performed where the species X was fixed in the center of the surface benzene. This allowed the proposed transition state to relax while still retaining the initial system symmetry. The potential endohedral candidates included NO. Nitric oxide is an interesting endohedral candidate since, as is true for the endohedral nitrogen atom, it is a radical and in the complex could provide many of the same spin properties that are so appealing in the nitrogen case. Nitric oxide, however, offers a practical advantage over the nitrogen atom in that the ground state is a doublet so that the added step of producing the radicals from stable molecules is eliminated. In the case of endohedral NO, the molecule was oriented with its intermolecular axis pointing directly at the center of the C_{60} cage. The oxygen atom was located in the

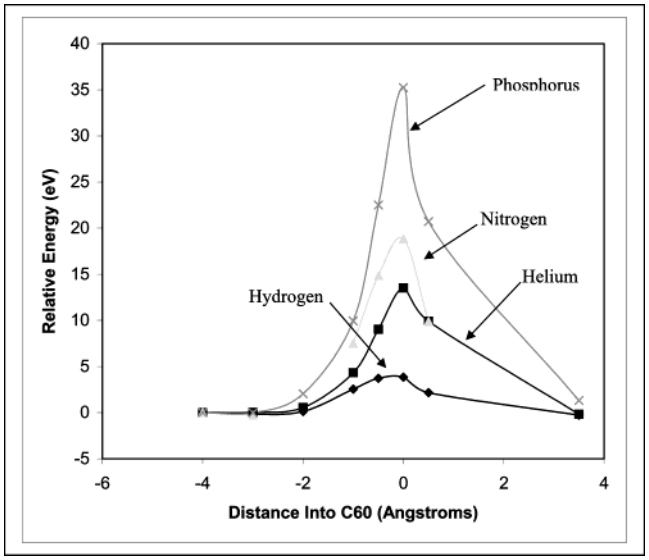

Figure 2. Potential energy curves with respect to X−C_{60} distance. In each case, the calculations used a fixed geometry transition state structure with a single relaxed surface C_6 ring. Calculations were performed using the B3LYP/6-31G(d) method.

TABLE 2: Energy Barriers for Formation of Endohedral C_{60}[a]

X	energy barrier, eV
H	3.84
He	13.53
N	18.86
P	35.23

[a] The transition state uses a *single* relaxed surface C_6 ring.

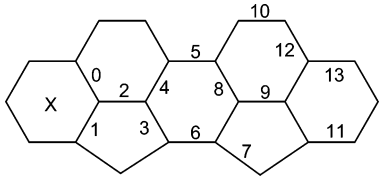

Figure 3. Schematic illustrating the symmetry-adapted bond-naming scheme used to identify reported bond lengths in this article.

center of the surface ring, with the nitrogen atom located further in toward the C_{60} center. Initially, the N−O bond distance was allowed to relax during the calculation. However, in the course of the optimization, the NO molecule began a process of complete dissociation, and the nitrogen atom moved to the center of the C_{60} cage. This dissociation may be the explanation for the absence of any experimental evidence of NO@C_{60}. For the final transition state geometries, the N−O bond distance has been arbitrarily fixed at its experimental value of 1.150 Å. This may be chemically unrealistic, but provides a molecular endohedral complex for comparative use in our study. The resultant optimized bond lengths, with the symmetry-adapted numbering convention for bonds contained in Figure 3, for all endohedral species are shown in Table 3.

Using this partially relaxed cage structure, B3LYP/6-31G* calculations were performed to determine an improved version of the potential energy barrier between the relaxed transition state and the isolated, separated species. These results, presented in Table 4, were determined by subtracting the potential energy at the point of noninteracting reactants from the transition state energy. As expected for this mechanism, the transition state energy barriers increase with increasing van der Waals radius of the monatomic species. Comparison of the results in Table 4, which represent energies of a partially optimized transition

TABLE 3: Optimized Bond Lengths for Each Endohedral Species, X[a]

bond	hydrogen	helium	nitrogen	phosphorus	arsenic	nitric oxide
0	1.3983	1.4449	1.5642	1.6386	1.6942	1.6363
1	1.4815	1.5402	1.5900	1.6340	1.6802	1.6894
2	1.4209	1.3866	1.3569	1.3216	1.3021	1.3065
3	1.4576	1.4799	1.5000	1.5064	1.5259	1.5281
4	1.3743	1.3693	1.4011	1.4156	1.4111	1.3992
5	1.4565	1.4554	1.4218	1.4094	1.4059	1.4207
6	1.3732	1.3498	1.3694	1.3590	1.3425	1.3187
7	1.4475	1.4567	1.4634	1.4706	1.4797	1.4892
8	1.3750	1.3726	1.4169	1.4197	1.4297	1.4313
9	1.4569	1.4574	1.4505	1.4465	1.4544	1.4531
10	1.3834	1.3731	1.4010	1.4076	1.3953	1.3766
11	1.3744	1.3755	1.4032	1.4248	1.4230	1.4166
12	1.4477	1.4611	1.4610	1.4708	1.4859	1.4773
13	1.4560	1.4668	1.5064	1.5209	1.5173	1.4831

[a] Partial optimizations were performed using Hartree−Fock ab initio calculations with a 3-21G* basis set. In each case, C_{60} cage bond angles and dihedrals were fixed at their undistorted values; pentagonal angles 108° and hexagonal angles 120°. Dihedral angles with a 6,5 bond axis were fixed at 142.6°, while dihedral angles with a 6,6 bond axis were fixed at 138.2°.

TABLE 4: Predicted Energy Barriers to the Formation of Endohedral Fullerene Structures Using the Direct Insertion Mechanism[a]

X	energy barrier, eV
H	3.27
He	10.98
N	16.12
P	23.94
As	30.27
NO	31.40

[a] All transition state structures have undergone partial geometry optimizations involving fourteen unique C_{60} bond lengths.

structure with those in Table 2, representing optimization of an only single hexagonal ring, show surprisingly good agreement for the smallest endohedral atoms. The estimated barriers for hydrogen atoms are nearly identical in the two cases, a result of the small-sized atom passing through an essentially undisturbed fullerene. The barriers in Table 2 are approximately 2 eV greater than those in Table 4 for nitrogen and helium atoms and, while the change in computational method doubtlessly plays a role, this difference also reflects the importance of the complete optimization of all bond lengths. The most optimistic interpretation of the barriers indicates that only H, He, and N are potential candidates for the insertion mechanism. The significant energy barriers of the larger species (and perhaps nitrogen) cast doubt that complex formation could occur by this mechanism for these atoms. For these species, formation would occur through a different mechanism, for example, the windowing or hole processes.

Windowing Mechanism. Table 4 indicates that the energy barrier for direct insertion of a nitrogen atom into C_{60} is ∼16 eV. While such a barrier may be surmounted in a high energy beam−surface impact system, this is a significant amount of energy and reflects the fact that the nitrogen atom is too large to easily pass through the fullerene surface without a substantial change in the geometry of the fullerene. As an alternative to the insertion mechanism, we explored the windowing process and, in particular, searched for a transition structure along the adiabatic approach of the endohedral atom to the fullerene. To determine the reaction pathway for the windowing mechanism, the endohedral atom and the fullerene are initially placed at a separation that ensures no interaction. The atom is moved toward the fullerene by a small increment and the system is structurally optimized. This optimized geometry is then used as the starting point for the next calculation at a new, smaller separation. The optimization is continued in this manner until the atom is located at its stationary point within the fullerene cage. Due to the large number of electrons, the semiempirical PM3 method is used for the generation of the potential energy as a function of separation with complete optimization. This search was successfully concluded for both hydrogen and nitrogen atoms, and the results are indicative of the possible assignment of this mechanism to the formation of these two complexes. Energy profiles for hydrogen and nitrogen are shown in Figure 4 along with important structural configurations at the relevant inflection points in the profiles. Reaction progress is indicated as distance of the approaching atom from the center of the fullerene. The cage center is set to 0 Å; therefore, the fullerene surface is at approximately 3.4 Å.

Consider first the hydrogen profile. As the hydrogen atom approaches the fullerene, there is the expected long range attraction that lowers the energy of the system. At approximately 5 Å from the fullerene center, a very loose bond is formed to a single carbon atom of the C_{60} cage and the energy begins to increase as the carbon−hydrogen distance is further decreased. At a separation of approximately 3.7 Å (∼0.3 Å from the fullerene shell), the bond begins to break. Finally, the atom passes through the ring and moves toward the center of the fullerene cage. The barrier for this process, which is essentially identical to direct insertion (there is no significant carbon−carbon bond expansion at the top of the barrier), is 3.01 eV which compares quite well to the barrier cited in Table 4, 3.27 eV.

The nitrogen atom energy profile is more complicated. The long range attraction as the nitrogen atom approaches from infinite separation leads to an initial, weak bond forming at approximately 5 Å from the center of the cage or ∼1.6 Å from the fullerene shell. The energy of the system increases as the bond distance is compressed, until at 4.8 Å another local minimum energy configuration is attained when the nitrogen atom bridges two carbons. Again, the energy increases until approximately 3.7 Å, when the nitrogen is inserted into a 6,5 carbon−carbon bond leading to a local energy minimum for the addition product with a puckered shell geometry. At ∼2 Å, the bridging bond has flipped completely inward, the 6,5 carbon−carbon bond reforms, and the nitrogen continues on toward the global energy minimum at the center of the fullerene. One of the bridging bonds breaks at ∼1.5 Å from the center of the cage, and the energy increases once more until the final bond breaks and the nitrogen atom reaches its global minimum energy position at the center of the cage. The barrier is estimated from the plot to be 5.72 eV, considerably less than that for direct insertion, ∼16 eV.

The larger radii of the phosphorus and arsenic atoms preclude optimization of a transition structure for this mechanism. The large size, substantial atomic polarizability, and the absence of translational energy in the calculation allow the phosphorus (or arsenic) to insert into the cage itself, creating a heterofullerene and ejecting a carbon atom. These negative results do not imply the absence of a windowing mechanism for these two endohedral species, but point to the need for energetic impact to overcome the tendency to interact more strongly with the carbon shell of the C_{60}.

Mechanistic Comparison. The results obtained from the current calculations are consistent with the related information available in the literature. For example, Hirsch et al.[5] have shown computationally that the endohedral nitrogen atom escapes the

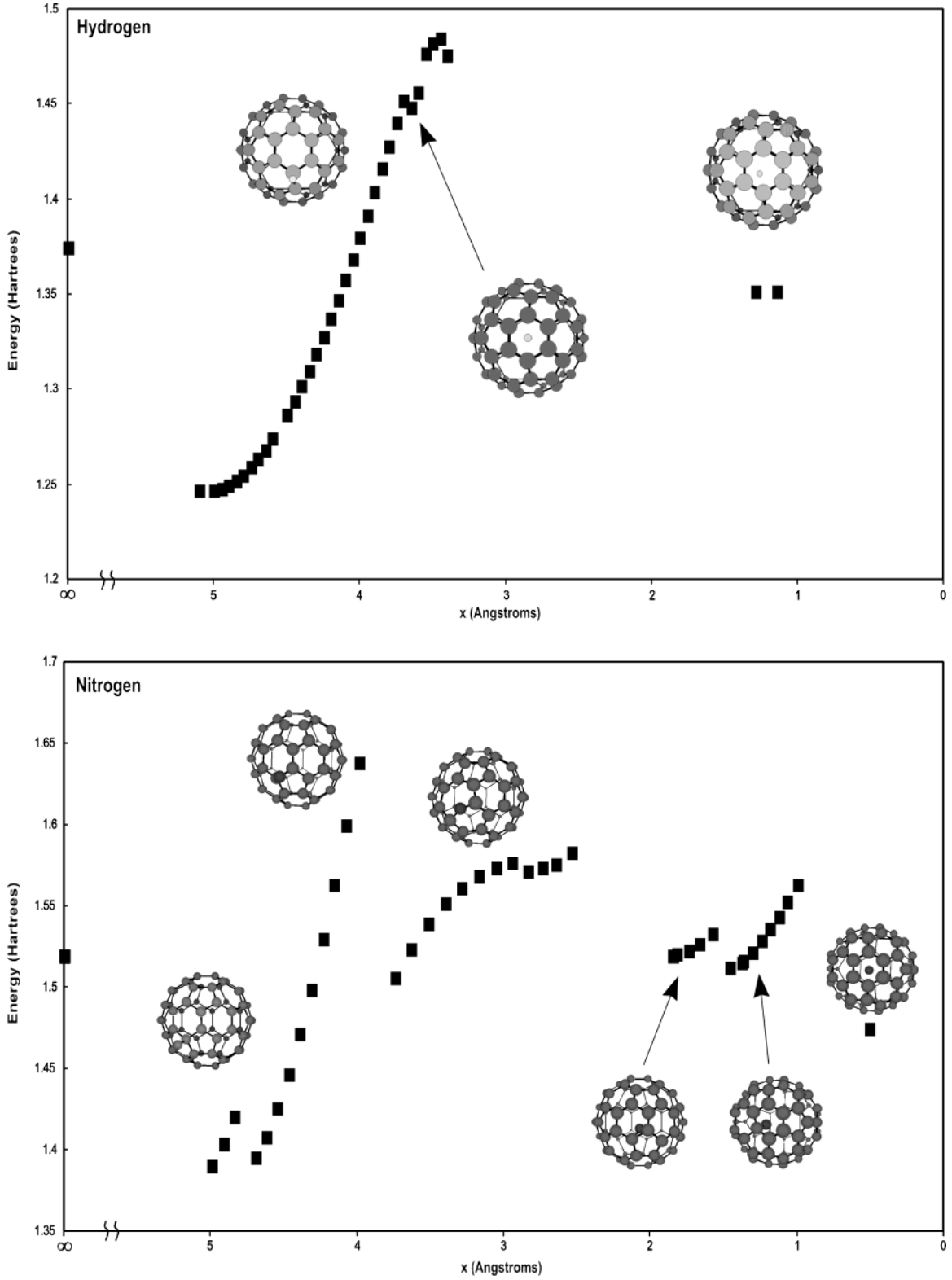

Figure 4. Energy profiles for the adiabatic approach of the endohedral atom toward the fullerene. Fully relaxed structures at each separation were calculated via the PM3 model.

fullerene cage after the formation of endohedral or aza bridges. This mechanism is essentially the windowing mechanism, proposed here, occurring in reverse sequence. The escape mechanism developed by Hirsch was shown to predict a lower nitrogen escape barrier in comparison to what would be expected for a direct loss of nitrogen, via the reverse of the insertion process. Experimentally, very mild temperature conditions (260 °C) were required to drive out the endohedral nitrogen atom, providing confirmation of the proposed escape mechanism. Our calculations indicate that the insertion barrier for nitrogen atoms is less than 6 eV for windowing, considerably smaller than our predicted barrier of ∼16 eV for direct insertion and in agreement with the observed experimental barrier[16] of 5.72 eV for nitrogen escape.

Also by considering the endohedral dissociation process, Lifshitz has shown[10] that the barrier for the C_2 shrink-wrap loss

mechanism is approximately 10 eV and that dissociation requires heating to ~1000 K for many hours. Since this dissociation process occurs preferentially over simple helium escape, the barrier for the latter must be greater than 10 eV. Our predicted formation barrier for direct helium insertion, nearly 11 eV, is mechanistically consistent with this previous research. Direct experimental measurements[16] for the loss of nitrogen or helium have confirmed the computational predictions. In both the nitrogen and helium compounds, our computational results are in excellent agreement with experimental findings.

Summary

On the basis of a combination of semiempirical, ab-initio and density functional theory calculations, possible transition structures for the formation of endohedral C_{60} complexes have been proposed. The proposed structures were those expected for the direct insertion and windowing mechanisms. For the former, transition state structures were obtained using partial geometry optimizations with the Hartree−Fock formalism and a small basis set. This yielded theoretical values for the energy barriers for formation of $X@C_{60}$, where X = H, He, N, NO, P, and As. Direct insertion was deemed possible for H, He, and (possibly) N with calculated barriers of 3.27 eV, 10.98 eV, and 16.12 eV, respectively. The extremely high energy barriers of P, As, NO, and possibly N suggest that formation of these endohedral C_{60} molecules may proceed more readily by a different mechanism, and therefore, through a different transition structure that is lower in energy. The possible transition structure for the windowing mechanism was examined for all endohedral species using a semiempirical (PM3) approach with complete optimization. On the basis of the computed energy barriers, the mechanism was found to be plausible for H and N with calculated barriers of 3.01 eV and 5.72 eV, respectively. The remaining systems would not converge to structures with endohedral atoms, but instead formed heterofullerenes. Insight into the molecular level formation process of endohedral complexes was provided by these calculations.

References and Notes

(1) Pietzak, B.; Waiblinger, M.; Murphy, T. A.; Weidinger, A.; Hoehne, M.; Dietal, E.; Hirsch, A. *Chem. Phys. Lett*. **1997**, *279*, 259.

(2) Pietzak, B.; Waiblinger, M.; Murphy, T. A.; Weidinger, A.; Hoehne, M.; Dietal, E.; Hirsch, A. *Carbon* **1998**, *36*, 613.

(3) Weidinger, A.; Pietzak, B.; Waiblinger, M.; Lips, K.; Nuber, B.; Hirsch, A. In *Electronic Properties of Novel Materials*; Kuzmany, H., et al., Eds.; American Institute of Physics, 1998.

(4) Weidinger, A.; Waiblinger, M.; Pietzak, B.; Murphy, T. A. *Appl. Phys*. **1998**, *A66*, 287.

(5) Mauser, H.; van Eikema Hommes, N. J. R.; Clark, T.; Hirsch, A.; Pietzak, B.; Weidinger, A.; Dunsch, L. *Angew. Chem., Int. Ed*. **1997**, *36*, 2835.

(6) BelBruno, J. J. *Fullerenes, Nanotubes, Carbon Nanostructures* **2002**, *10*, 23.

(7) Smith, R.; Beardmore, K.; BelBruno, J. *J. Chem. Phys*. **1999**, *111*, 9227.

(8) Saunders, M.; Jimenez-Vasquez, H. A.; Cross, R. J.; Mroczkowski, S.; Gross, M. L.; Giblin, D. E.; Poreda, R. J. *J. Am. Chem. Soc*. **1994**, *116*, 2193.

(9) Giblin, D. E.; Gross, M. L.; Saunders: M.; Jimenez-Vasquez, H. A.; Cross, R. J. *J. Am. Chem. Soc*. **1997**, *119*, 9883.

(10) Lifshitz, C. *Int. J. Mass Spectrom.* **2000**, *198*, 1.

(11) Cui, F. Z.; Liao, D. X.; Li, H. D. *Phys. Lett. A* **1994**, *195*, 156.

(12) Hrusak, J.; Boehme, D. K.; Weiske, T.; Schwarz, H. *Chem. Phys. Lett.* **1992**, *193*, 97.

(13) Moran-Lopez, J. L.; Cabrera-Trujillo, J. M.; Dorantes-Davila, J. *Solid State Commun.* **1995**, *96*, 451.

(14) Murry, R. L.; Scuseria, G. E. *Science* **1994**, *263*, 791.

(15) Frisch, M. J.; Trucks, G. W.; Schlegel, H. B.; Scuseria, G. E.; Robb, M. A.; Cheeseman, J. R.; Zakrzewski, V. G.; Montgomery, J. A., Jr.; Stratmann, R. E.; Burant, J. C.; Dapprich, S.; Millam, J. M.; Daniels, A. D.; Kudin, K. N.; Strain, M. C.; Farkas, O.; Tomasi, J.; Barone, V.; Cossi, M.; Cammi, R.; Mennucci, B.; Pomelli, C.; Adamo, C.; Clifford, S.; Ochterski, J.; Petersson, G. A.; Ayala, P. Y.; Cui, Q.; Morokuma, K.; Malick, D. K.; Rabuck, A. D.; Raghavachari, K.; Foresman, J. B.; Cioslowski, J.; Ortiz, J. V.; Stefanov, B. B.; Liu, G.; Liashenko, A.; Piskorz, P.; Komaromi, I.; Gomperts, R.; Martin, R. L.; Fox, D. J.; Keith, T.; Al-Laham, M. A.; Peng, C. Y.; Nanayakkara, A.; Gonzalez, C.; Challacombe, M.; Gill, P. M. W.; Johnson, B. G.; Chen, W.; Wong, M. W.; Andres, J. L.; Head-Gordon, M.; Replogle, E. S.; Pople, J. A. *Gaussian 98*, revision A.11; Gaussian, Inc.: Pittsburgh, PA, 1998.

(16) Cao, B.; Cross, R. J.; Saunders: M.; Lifshitz, C. *J. Phys. Chem. A* **2001**, *105*, 2142.